

# Multi-Objective Fuzzy Optimization of Sizing and Location of Piezoelectric Actuators and Sensors

**Nemanja D. Zorić**

Teaching Assistant  
University of Belgrade  
Faculty of Mechanical Engineering

**Aleksandar M. Simonović**

Assistant Professor  
University of Belgrade  
Faculty of Mechanical Engineering

**Zoran S. Mitrović**

Full Professor  
University of Belgrade  
Faculty of Mechanical Engineering

**Slobodan N. Stupar**

Full Professor  
University of Belgrade  
Faculty of Mechanical Engineering

*This paper presents the multi-objective fuzzy optimization of sizing and location of piezoelectric actuators and sensors on the thin-walled composite beam for active vibration control, using the degree of controllability (DC) for controlled modes as optimization criteria. The optimization process is performed constraining the original dynamics properties change including the limitation of increase of the mass, using or neglecting the limitation in degrees of controllability for residual modes for reduction spillover effect. Pseudogoal functions derived on the fuzzy set theory gives a unique expression for global objective functions eliminating the use of penalty functions. The problem is formulated using the finite element method based on the third-order shear deformation theory. The particle swarm optimization technique is used to find optimal configuration. Several numerical examples are presented for the cantilever beam.*

**Keywords:** multi-objective optimization, fuzzy logic, piezoelectric sensor, actuator, particle swarm.

## 1. INTRODUCTION

Piezoelectric actuators and sensors have a wide range of applications in vibration suppression and shape control. The optimization of sizing and location of actuators and sensors for active vibration control of flexible structures has been shown as the one of the most important issues in the design of active structures since these parameters have a major influence on the performance of the control system [1,2]. The optimization problem can be divided into two approaches. The first approach consists of the combination of optimal location and size of sensors and actuators and controller parameters [3,4]. The second approach deals with optimal location and size of sensors and actuators independently of controller definition [5-7].

Many times, an active structure is discretized into a finite number of elements for vibration analysis and control. For practical implementation, this model needs to be truncated, where only the first few modes are taken into account. However, the state feedback control law, based on a reduced model, may excite the residual modes resulting with spillover instability for even simple beam problem [8]. Considering that fact, some authors involved residual modes in the optimization problem [6,9].

Due to the complexity of the problem, classical optimization methods that apply gradient-based search techniques are not convenient for use. A good solution for such optimization problems relies on heuristic optimization algorithms. Some studies have used genetic algorithm (GA) [6,10], and Simulated annealing

(SA) algorithm [11] for finding out the optimal sizing and location of sensors and actuators and other parameters related to the control performances.

This paper deals with the multi-objective fuzzy optimization of placement and sizing of collocated piezoelectric actuators and sensors on a composite beam for maximum active vibration control effectiveness. The optimization problem is formulated independently of controller definition using the DC to measure control effectiveness for the vibration in the controlled modes. Optimization criteria are used ensuring a good DC for the controlled modes. The optimization process is performed constraining the original dynamic properties change including the limitation of increase of the mass, using or neglecting the limitation in DCs for residual modes for spillover effect reduction. To the best of our knowledge, the multi-objective fuzzy optimization based on the particle swarm optimization technique will present an innovative approach for solving the problem of sizing and location of piezoelectric actuators and sensors. Both objective functions and constraints are evaluated by the membership function. In that way, the use of weighting coefficients and penalty functions are avoided.

## 2. FINITE ELEMENT MODEL

A laminated composite beam with integrated piezoelectric sensors and actuators is considered (Fig. 1). The coordinate  $x$  is coincident with the beam axis, the  $x - y$  plane coincides with a mid-plane of the beam and the  $z$  axis is defined as normal to the mid-plane according to the right-hand rule. Both elastic and piezoelectric layers are supposed to be thin, such that a plane stress state can be assumed. The sensors and actuators are perfectly bonded on the upper and lower surfaces at different locations along the length of the beam. It is assumed that they span the entire width of the beam. Elastic layers are obtained by setting their

Received: September 2011, Accepted: November 2011

Correspondence to: Nemanja Zorić  
Faculty of Mechanical Engineering,  
Kraljice Marije 16, 11120 Belgrade 35, Serbia  
E-mail: nzoric@mas.bg.ac.rs

piezoelectric coefficients to zero. The equivalent single layer theory is used, so the same displacement field is considered for all layers of the beam. The formulation results in a coupled finite element model with mechanical (displacement) and electrical (potentials of piezoelectric patches) degrees of freedom. Also, only specially orthotropic layers are considered.

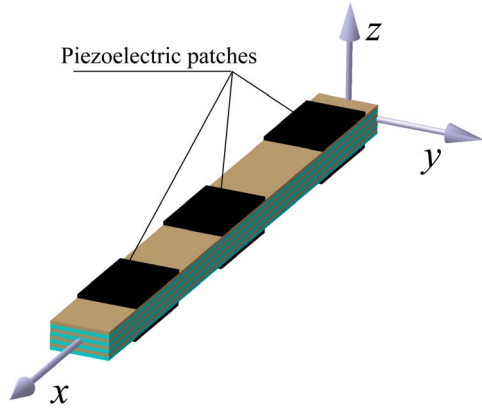


Figure 1. Laminated composite beam with piezoelectric sensors and actuators

## 2.1 Mechanical displacements and strains

The displacement field based on the third-order shear deformation theory of Reddy's [12] is given:

$$u(x, z, t) = u_0(x, t) + z\psi_x(x, t) - c_1 z^3 \left( \psi_x + \frac{\partial w_0}{\partial x} \right),$$

$$w(x, z, t) = w_0(x, t) \quad (1)$$

where  $u$  and  $w$  are displacement components in the  $x$  and  $z$  directions respectively,  $u_0$ ,  $w_0$  are mid-plane ( $z = 0$ ) displacement and  $\psi_x$  is bending rotation of mid-plane,  $c_1 = 4/(3h^2)$ , where  $h$  is total thickness of the beam. The strains associated with above displacement field are:

$$\varepsilon_{xx} = \varepsilon_{xx}^0 + z\varepsilon_{xx}^1 - c_1 z^3 \varepsilon_{xx}^3, \quad \gamma_{xz} = \gamma_{xz}^0 - c_2 z^2 \gamma_{xz}^2 \quad (2)$$

where

$$\varepsilon_{xx}^0 = \frac{\partial u_0}{\partial x}, \quad \varepsilon_{xx}^1 = \frac{\partial \psi_x}{\partial x}, \quad \varepsilon_{xx}^3 = \frac{\partial \psi_x}{\partial x} + \frac{\partial^2 w_0}{\partial x^2},$$

$$\gamma_{xz}^0 = \gamma_{xz}^2 = \psi_x + \frac{\partial w_0}{\partial x} \quad (3)$$

and

$$c_2 = \frac{4}{h^2}. \quad (4)$$

## 2.2 Piezoelectric constitutive equations

Specific electric enthalpy density of a piezoelectric layer is given in [13]:

$$h = \frac{1}{2} \{\varepsilon\}^T [Q] \{\varepsilon\} - \{\varepsilon\}^T [e] \{E\} - \frac{1}{2} \{E\}^T [k] \{E\}, \quad (5)$$

where  $[Q]$  is the elastic stiffness matrix,  $\{\varepsilon\}$  is the strain vector,  $[e]$  is the piezoelectric constant matrix,  $\{E\}$  is

the electric field vector and  $[k]$  is the permittivity matrix. Therefore, the constitutive equations for each piezoelectric layer can be obtained:

$$\{\sigma\} = \frac{\partial h}{\partial \{\varepsilon\}} = [Q] \{\varepsilon\} - [e]^T \{E\},$$

$$\{D\} = -\frac{\partial h}{\partial \{E\}} = [e] \{\varepsilon\} + [k] \{E\} \quad (6)$$

where  $\{\sigma\}$  is the stress vector and  $\{D\}$  is the electric displacement vector. For a one-dimensional composite beam, the width ( $y$ -direction) is free of stresses. Therefore,  $\sigma_y = \sigma_{yz} = \sigma_{xy} = 0$  and  $\varepsilon_y \neq \gamma_{yz} \neq \gamma_{xy} \neq 0$ . Using the above constraints, assuming that  $E_1 = E_2 = 0$  and taking into account specially orthotropic laminate which consists of  $n$  layers, constitutive equation for  $k$ -th layer can be written as:

$$\begin{Bmatrix} \sigma_{xx} \\ \sigma_{xz} \\ D_3 \end{Bmatrix}^{(k)} = \begin{bmatrix} \bar{Q}_{11} & 0 & -\bar{e}_{31} \\ 0 & \bar{Q}_{55} & 0 \\ -\bar{e}_{31} & 0 & \bar{k}_{33} \end{bmatrix}^{(k)} \begin{Bmatrix} \varepsilon_{xx} \\ \gamma_{xz} \\ E_3 \end{Bmatrix}^{(k)}, \quad (7)$$

where material constants are expressed in principal directions. Relations between material constants expressed in the principal direction and material directions for orthotropic lamina are:

$$\bar{Q}_{11} = Q_{11} \cos^4 \Theta + Q_{22} \sin^4 \Theta,$$

$$\bar{Q}_{55} = Q_{55} \cos^2 \Theta + Q_{44} \sin^2 \Theta,$$

$$\bar{e}_{31} = e_{31} \cos^2 \Theta + e_{32} \sin^2 \Theta,$$

$$\bar{k}_{33} = k_{33} \quad (8)$$

where  $\Theta$  presents an angle between the material directions of the layer and the principal direction of the lamina.

## 2.3 Finite element discretization and coupled equations of motions

After finite element discretization [11], global equations of motions can be written in terms of the nodal mechanical and electrical degrees of freedom as:

$$[M] \{\ddot{u}\} + [K_m] \{u\} + [K_{me}]_A \{\phi\}_A + [K_{me}]_S \{\phi\}_S = \{F_m\},$$

$$[K_{me}]_A^T \{u\} - [K_e]_A \{\phi\}_A = [K_e]_A \{\phi\}_{AA},$$

$$[K_{me}]_S^T \{u\} - [K_e]_S \{\phi\}_S = 0, \quad (9)$$

where  $[M]$  presents mass matrix,  $[K_m]$  presents elastic stiffness matrix,  $[K_{me}]_A$  and  $[K_{me}]_S$  are piezoelectric stiffness matrices of actuator and sensor, respectively,  $[K_e]_A$  and  $[K_e]_S$  are dielectric stiffness matrices of actuator and sensor, respectively,  $\{u\}$  presents vector of mechanical nodal variables,  $\{\phi\}_A$  and  $\{\phi\}_S$  are electric potentials on actuators and sensors, respectively and  $\{\phi\}_{AA}$  is vector of external applied electric potentials on actuators.  $\{F_m\}$  presents vector of external forces. From (9), it can be obtained the following equation of motion:

$$[M] \{\ddot{u}\} + [K^*] \{u\} = \{F_m\} + [K_{me}]_A \{\phi\}_{AA}, \quad (10)$$

where:

$$[K^*] = [K_m] + [K_{me}]_A [K_e]_A^{-1} [K_{me}]_A^T + [K_{me}]_S [K_e]_S^{-1} [K_{me}]_S^T. \quad (11)$$

## 2.4 Modal form and state-space representation

Equation (10) can be converted to modal-space as:

$$\{\ddot{\eta}\} + [\omega^2] \{\eta\} = [\Psi]^T \{F_m\} + [\Psi]^T [K_{me}]_A \{\phi\}_{AA}, \quad (12)$$

where  $\Psi$  presents modal matrix which has been normalized with respect to mass,  $\{\eta\}$  vector of modal coordinates and  $[\omega^2]$  diagonal matrix of squares natural frequencies obtained in following way:

$$[\omega^2] = [\Psi]^T [K^*] [\Psi]. \quad (13)$$

Lower ordered modes are the most easily excitable because they have lower energy associated. Due to that, a controller has been designed for active control for only first few modes. Thus, (12), expressed in truncated modal-space, becomes:

$$\{\ddot{\eta}\} + [\omega^2]_C \{\eta\} = [\Psi]_C^T \{F_m\} + [\Psi]_C^T [K_{me}]_A \{\phi\}_{AA}, \quad (14)$$

where matrix  $[\omega^2]_C$  is consisted of first few controlled eigen-modes. For residual modes, (12) becomes:

$$\{\ddot{\eta}\} + [\omega^2]_R \{\eta\} = [\Psi]_R^T \{F_m\} + [\Psi]_R^T [K_{me}]_A \{\phi\}_{AA}. \quad (15)$$

Equations (14) and (15) can be presented in state-space form as:

$$\{\dot{X}\} = [A] \{X\} + [B] \{\phi\}_{AA} + \{d\}, \quad (16)$$

where

$$\{X\} = \begin{Bmatrix} \{\eta\} \\ \{\dot{\eta}\} \end{Bmatrix} \quad (17)$$

presents state vector,

$$[A] = \begin{bmatrix} [0] & [0] & [I] & [0] \\ [0] & [0] & [0] & [I] \\ -[\omega^2]_C & [0] & [0] & [0] \\ [0] & -[\omega^2]_R & [0] & [0] \end{bmatrix} \quad (18)$$

presents state matrix,

$$[B] = \begin{bmatrix} [0] \\ [0] \\ [B]_C \\ [B]_R \end{bmatrix} = \begin{bmatrix} [0] \\ [0] \\ [\Psi]_C^T [K_{me}]_A \\ [\Psi]_R^T [K_{me}]_A \end{bmatrix} \quad (19)$$

presents control matrix, and

$$\{d\} = \begin{Bmatrix} \{0\} \\ \{0\} \\ [\Psi]_C^T \{F_m\} \\ [\Psi]_R^T \{F_m\} \end{Bmatrix} \quad (20)$$

is disturbance vector, where  $[I]$  and  $[0]$  are appropriately dimensioned identity and zero matrix, respectively.

## 3. OPTIMIZATION CRITERIA FOR COLLOCATED PIEZOELECTRIC ACTUATORS AND SENSORS SIZING

### 3.1 Multi-objective optimization problem statement

In [14], a controllability index for actuator is proposed, which is obtained by maximizing the global control force. The modal control force applied to the system can be written as:

$$\{f_C\} = [B] \{\phi\}_{AA}. \quad (21)$$

It follows from (21) that

$$\{f_C\}^T \{f_C\} = \{\phi\}_{AA}^T [B]^T [B] \{\phi\}_{AA}. \quad (22)$$

Using singular value analysis,  $[B]$  can be written as  $[B] = [M][S][N]^T$ , where  $[M]^T[M] = [I]$ ,  $[N]^T[N] = [I]$  and

$$[S] = \begin{bmatrix} \sigma_1 & 0 & \dots & 0 \\ 0 & \sigma_2 & & 0 \\ \vdots & & \ddots & \vdots \\ 0 & 0 & \dots & \sigma_{N_A} \\ \vdots & \vdots & & \vdots \\ 0 & 0 & \dots & 0 \end{bmatrix}, \quad (23)$$

where  $N_A$  presents the number of actuators. Equation (22) can be written as:

$$\{f_C\}^T \{f_C\} = \{\phi\}_{AA}^T [N]^T [S]^T [S] [N] \{\phi\}_{AA} \quad (24)$$

or

$$\|f_C\|^2 = \|\phi\|_{AA}^2 \|S\|^2. \quad (25)$$

Thus, maximizing this norm independently of the applied voltage  $\{\phi\}_{AA}$  induces maximizing  $\|S\|^2$ . The magnitude of  $\sigma_i$  is a function of location and size of piezoelectric actuator. In [14] the proposed controllability index which is defined by:

$$\Omega_C = \prod_{i=1}^{N_A} \sigma_i. \quad (26)$$

The higher controllability index, the smaller electrical potential will be required for control. This index represents controllability for all the modes globally, and its magnitude is a function of the location and size of the piezoelectric actuators. The lack of this definition of controllability index is in fact that it gives only information of controllability for all modes of all actuators, i.e. it can not be seen controllability for a certain mode. Controllability index can be obtained in a more suitable form for models based on finite element, where, instead of maximizing the norm  $\|S\|^2$ , the applied force for each mode have been maximized independently of  $\{\phi\}_{AA}$ . According to (19), the controllability index can be written in the following way:

$$\bar{\sigma}_{C_i}^2 = (B_i)_C (B_i)_C^T \quad (27)$$

for controlled mode, and

$$(\bar{\sigma}_{C_i}^R)^2 = (B_i)_R (B_i)_R^T \quad (28)$$

for residual mode.  $(B_i)_C$  and  $(B_i)_R$  present  $i$ -th row of matrices  $[B]_C$  and  $[B]_R$ , respectively.

As mentioned earlier, the piezoelectric patches sizing and location should be such that those should give good controllability for controlled modes, so the objective functions can be written as:

$$\text{maximize } DC_{C_i} = \frac{\bar{\sigma}_{C_i}^2}{\bar{\sigma}_{C_i \max}^2} \cdot 100, \quad i = 1, \dots, N_C, \quad (29)$$

where  $DC_{C_i}$  presents the degree of controllability (DC) for controlled modes,  $\bar{\sigma}_{C_i \max}$  denotes the maximum controllability index for controlled modes and  $N_C$  presents the number of controlled modes. It is shown that misplaced sensors and actuators lead to control system instability [15]. Due to that, in this work, only collocated sensors and actuators will be considered. The actuator and its corresponding sensor have equal length and they are set symmetrically: sensor at the bottom surface, and actuator on the top surface of the beam.

### 3.2 Constraints

Constraints are related to the change of natural frequencies and mass of parent structure and DC of residual modes. They can be written as follows:

$$\left| \frac{\omega_i^* - \omega_i}{\omega_i} \right| < \varepsilon_{fi}, \quad i = 1, \dots, N_{f \text{ mods}}, \quad (30)$$

$$\left| \frac{m^* - m}{m} \right| < \varepsilon_m, \quad (31)$$

$$DC_{R_i} < DC_{R_i}^{\max}, \quad i = 1, \dots, N_R, \quad (32)$$

where  $\omega_i^*$  denotes natural frequency of the  $i$ -th mode of the beam with piezoelectric patches,  $\omega_i$  denotes natural frequency of the  $i$ -th mode of the beam without piezoelectric patches,  $\varepsilon_{fi}$  is tolerance of change of the  $i$ -th natural frequency,  $N_{f \text{ mods}}$  presents the number of constrained modes,  $m^*$  denotes mass of the beam with piezoelectric patches,  $m$  denotes mass of the parent beam and  $\varepsilon_m$  is tolerance of the mass change and  $DC_{R_i}^{\max}$  denotes the maximum allowable DC for the  $i$ -th residual mode.

### 3.3 Mathematical model of multi-objective fuzzy optimization

In this section, a fuzzy optimization approach based on pseudogoal function for the multi-objective problem is proposed. The objective functions (29), which have to be maximized, can be written as the pseudogoal function in the form of the fuzzy number:

$$\mu_{C_i}(\mathbf{p}) = \frac{DC_{C_i}(\mathbf{p}) - DC_{C_i \min}}{DC_{C_i \max} - DC_{C_i \min}}, \quad (33)$$

where  $DC_{C_i \min}$  and  $DC_{C_i \max}$  denote the minimum and maximum DC for controlled modes, respectively,  $\mu_{C_i}(\mathbf{p})$  presents the membership function of the  $i$ -th objective function and  $\mathbf{p}$  presents the design variables set. According to the formulation of DC ( $DC_{C_i \min} = 0$  and  $DC_{C_i \max} = 100$ ), previous expression becomes (Fig. 2a):

$$\mu_{\text{Cont}_i}(\mathbf{p}) = \frac{DC_{C_i}(\mathbf{p})}{100}. \quad (34)$$

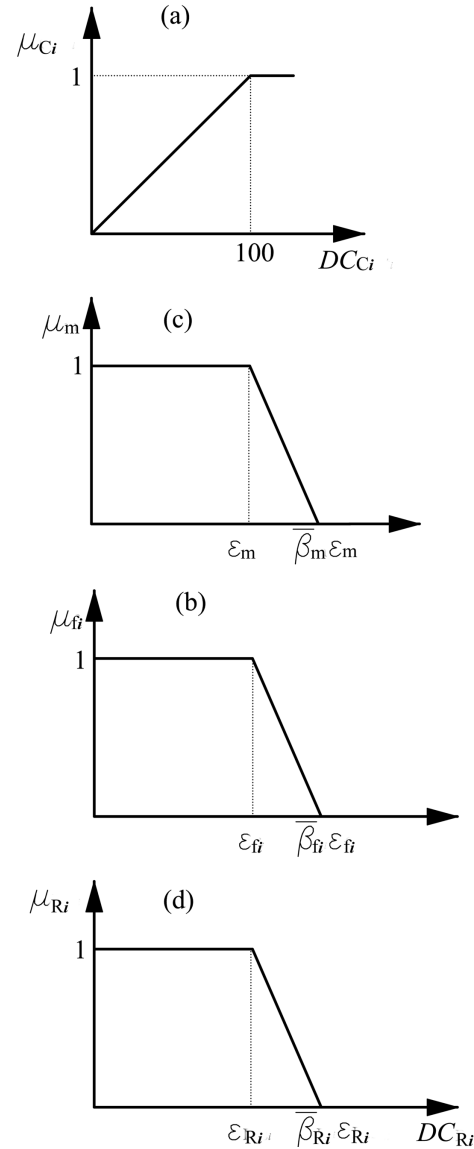


Figure 2. Membership functions of objective functions and constraints

Constraints may also receive the same fuzzification process as the objective functions. In this process, the amplification method [16] is used. This method is often used in engineering to determine the tolerance of the upper limit of the constraints. Usually, the value of this coefficient is  $\bar{\beta} = 1.05 - 1.3$ . So, the membership functions of constraints become (Figs. 2b, 2c and 2d):

$$\mu_{f_i}(\mathbf{p}) = \left\{ \begin{array}{l} 1, \quad \frac{|\omega_i^* - \omega_i|}{\omega_i} < \varepsilon_{fi} \\ \frac{\bar{\beta}_{f_i} \varepsilon_{fi} - \frac{|\omega_i^* - \omega_i|}{\omega_i}}{\bar{\beta}_{f_i} \varepsilon_{fi} - \varepsilon_{fi}}, \quad \varepsilon_{fi} \leq \frac{|\omega_i^* - \omega_i|}{\omega_i} < \bar{\beta}_{f_i} \varepsilon_{fi} \\ 0, \quad \frac{|\omega_i^* - \omega_i|}{\omega_i} \geq \bar{\beta}_{f_i} \varepsilon_{fi} \end{array} \right\}, \quad (35)$$

$$\mu_m(\mathbf{p}) = \left\{ \begin{array}{l} 1, \quad \frac{|m^* - m|}{m} < \varepsilon_m \\ \frac{\bar{\beta}_m \varepsilon_m - \frac{|m^* - m|}{m}}{\bar{\beta}_m \varepsilon_m - \varepsilon_m}, \quad \varepsilon_m \leq \frac{|m^* - m|}{m} < \bar{\beta}_m \varepsilon_m \\ 0, \quad \frac{|m^* - m|}{m} \geq \bar{\beta}_m \varepsilon_m \end{array} \right\}, \quad (36)$$

$$\mu_{R_i}(\mathbf{p}) = \left\{ \begin{array}{l} 1, \quad DC_{R_i} < DC_{R_i}^{\max} \\ \frac{\bar{\beta}_R DC_{R_i}^{\max} - DC_{R_i}}{\bar{\beta}_R DC_{R_i}^{\max} - DC_{R_i}^{\max}}, \quad DC_{R_i}^{\max} \leq DC_{R_i} < \bar{\beta}_R DC_{R_i}^{\max} \\ 0, \quad DC_{R_i} \geq \bar{\beta}_R DC_{R_i}^{\max} \end{array} \right\}. \quad (37)$$

According to the fuzzy decision principle proposed in [17], the fuzzy decision is defined as the intersection of fuzzy objectives and fuzzy constraints. Thus, the optimum solution  $\mathbf{p}^*$  can be selected by maximizing the smallest membership function:

$$\mu_D(\mathbf{p}^*) = \max \mu_D(\mathbf{p}), \quad (38)$$

where

$$\mu_D = \min \{ \mu_{C_i}, \mu_{f_j}, \mu_m, \mu_{R_k} \} \quad (39)$$

presents the membership function of the optimal decision function.

#### 4. OPTIMIZATION IMPLEMENTATION USING PARTICLE SWARM OPTIMIZATION

The particle swarm optimization (PSO) has been inspired by the social behaviour of animals such as fish schooling, insect swarming and birds flocking. It was introduced in [18]. The system is initialized with a population of random solutions (called the particle position in PSO). Every particle is affected by three

factors: its own velocity, the best position it has achieved (best local position) which is determined by the highest value of the objective function encountered by this particle in all previous iteration and overall best position achieved by all particles (best global position), which is determined by the highest value of the objective function encountered in all the previous iteration. A particle changes its velocity ( $v$ ) and position ( $p$ ) in the following way:

$$v_{id}^{k+1} = wv_{id}^k + c_1r_1(l_{id} - p_{id}^k) + c_2r_2(g_d - p_{id}^k), \quad (40)$$

$$p_{id}^{k+1} = p_{id}^k + v_{id}^{k+1}, \quad i = 1, \dots, n, \quad d = 1, \dots, m, \quad (41)$$

where  $w$  is inertia weight,  $c_1$  is cognition factor,  $c_2$  is social learning factor,  $r_1$  and  $r_2$  are random numbers between 0 and 1, the superscript  $k$  denotes iterative generation,  $n$  is population size,  $m$  is particle's dimension,  $l_{id}$  and  $g_d$  are best local and global position. The cognition factor and social learning factor are usually set as  $c_1 = c_2 = 1.5$ . The upper and lower limits of inertia weight for structural design are given in [19]. Each S/A pair is determined by two parameters: the position which presents the distance from the root of the beam ( $r$ ) and their length ( $l$ ) (Fig. 3a). In this work, the beam is discretized in finite elements, so, the position of S/A pair is defined by the position of left node and the length is defined by the number of elements covered by this pair (Fig. 3b). According to the previous,  $p_{i(2j-1)}^k$  presents the position of the  $j$ -th S/A pair, and  $p_{i(2j)}^k$  presents its length.

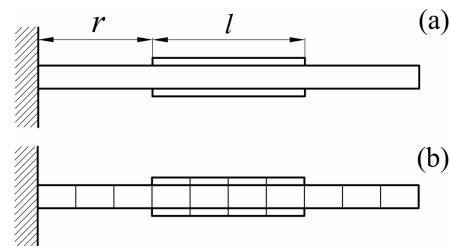


**Figure 3. (a) position and length of arbitrary S/A pair on beam and (b) position and length of arbitrary S/A pair after discretization**

It is obvious that coordinates of the particle and corresponding velocity are an integer number. Because of that, the discrete method must be used. According to [20], the velocity is updated by the following equation on every iteration:

$$v_{id}^{k+1} = \text{int}(wv_{id}^k + c_1r_1(l_{id} - p_{id}^k) + c_2r_2(g_d - p_{id}^k)), \quad (42)$$

in which  $\text{int}(f)$  is getting an integer part of  $f$ . Due to the formulation of the coordinates of a particle, other constraints appear – the geometric constraints. These constraints are:

- the coordinates of the particle must not be a non-positive number;
- the minimum distance between two patches is one element (there is no overlapping);
- the last piezoelectric patch must not be outside of the beam.

The membership function of this constraint can be represented in the following way

$$\mu_G = \begin{cases} 1, & \text{if geometric constraints are not violated} \\ 0, & \text{if geometric constraints are violated} \end{cases} \quad (43)$$

and optimization problem can be transformed on following way

$$\mu_D(\mathbf{p}^*) = \max \mu_D(\mathbf{p}), \quad (44)$$

where

$$\mu_D = \min \{ \mu_{C_i}, \mu_{f_j}, \mu_m, \mu_{R_k}, \mu_G \}. \quad (45)$$

## 5. NUMERICAL EXAMPLE

In this example, the cantilever laminated beam is considered. The length of beam is 0.6 m, and its width is 0.03 m. The beam is made of seven graphite-epoxy (carbon-fibre reinforced) layers. The thickness of each layer is 0.5 mm and orientations are  $(90^0/90^0/0^0/0^0/0^0/90^0/90^0)$ . Piezoelectric patches are made of PZT. Their thicknesses are 0.2 mm. Material properties of graphite-epoxy and PZT are given in table 1.

**Table 1. Material properties of graphite-epoxy and PZT**

Material properties	Graphite-epoxy	PZT
$E_1$ [GPa]	174	63
$E_2$ [GPa]	10.3	63
$G_{13}$ [GPa]	7.17	24.6
$G_{23}$ [GPa]	6.21	24.6
$\nu_{12}$	0.25	0.28
$\rho$ [kg/m <sup>3</sup> ]	1389.23	7600
$e_{31}$ [C/m <sup>2</sup> ]	–	10.62
$k_{33}$ [F/m]	–	$0.1555 \cdot 10^{-7}$

The beam is discretized in 60 elements. The first five modes are considered as controlled modes, and the next five modes are used to reduce the spillover effect. As mentioned earlier, the mounting piezoelectric sensor/actuator pairs cause changes of the original dynamic properties and mass of parent structure. Table 2 shows natural frequencies of the first ten modes of parent beam and maximum change of natural frequencies after mounting of piezoelectric S/A pairs.

**Table 2. Natural frequencies of parent beam, maximum value of natural frequencies after mounting S/A pairs and maximum change of natural frequencies after mounting of S/A pairs**

Mode	Natural frequency of parent beam [Hz]	Maximum value of natural frequencies after mounting S/A pairs [Hz]	Maximum NF change [%]
1	6.437	9.189	42.755
2	40.347	50.545	25.277
3	113.014	137.879	22.002
4	221.573	267.361	20.665
5	366.513	439.328	19.867
6	547.942	653.635	19.289
7	766.030	910.748	18.892
8	1020.962	1209.595	18.476
9	1313.008	1549.875	18.040
10	1642.389	1931.187	17.584

The mass of beam without S/A pairs is 0.0875 kg, and the mass of beam fully covered by S/A pairs is 0.1422 kg, resulting in the maximum change of mass that is 62.56 %.

In the optimization problem, the numbers of S/A pairs are varied from one to three. Two examples for every number of S/A pairs are done: one without limit of the spillover effect, and other, where the spillover effect is considered to be less than 2 % with tolerance of the upper limit  $\bar{\beta}_{Rez_i} = 1.1$ . Changes of the first five natural frequencies are less than 10 %, and the mass change is less than 15 % with tolerance of the upper limit  $\bar{\beta}_{f_i} = \bar{\beta}_m = 1.15$ .

In order to search efficiently for the optimal sizing and location of S/A pairs, the cognition and social learning factors in PSO algorithm are set as  $c_1 = c_2 = 1.5$ , and inertia weights are linearly varied from 1 to 0.5. The number of population is 30 particles, and the number of iteration is 50.

Numbers of S/A pairs are varied from one to three. Figure 4 shows the objective function value against the number of iteration for the case of one S/A pair. Figures 5 – 10 present the location and length of S/A pairs and DCs for the first ten modes for unconstrained (Figs. 5, 7 and 9) and constrained (Figs. 6, 8 and 10) DCs for residual modes, in case of one, two and three S/A pairs, respectively. Table 3 presents the optimal sizes and locations of one, two and three S/A pairs.

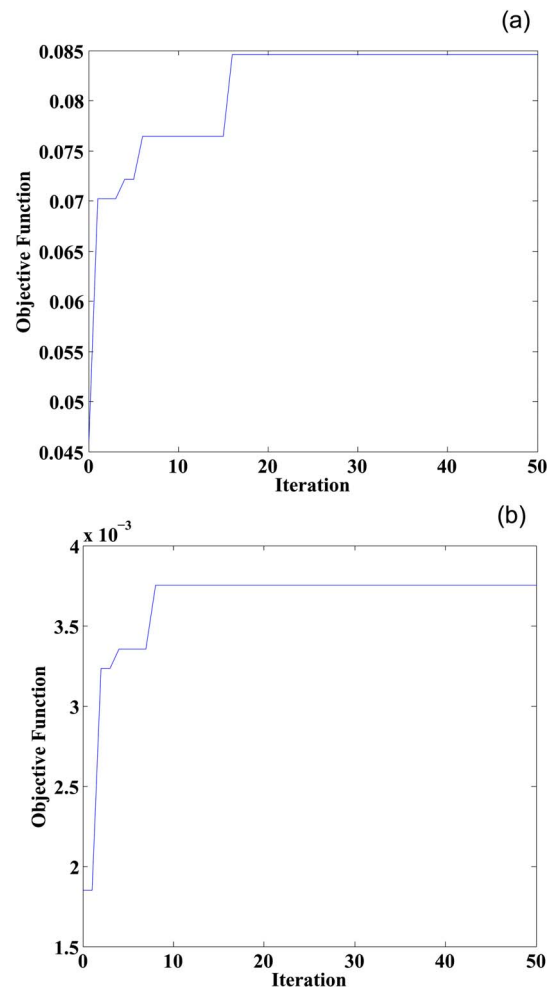


**Figure 4. The objective function value against number of iteration for single S/A pair: (a) unconstrained DC for residual modes and (b) DC for residual modes less than 2 %**

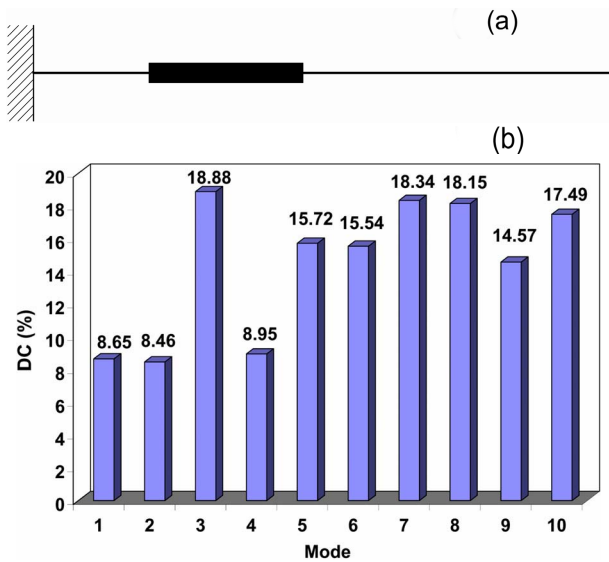


Figure 5. Single S/A pair, unconstrained DC for residual modes: (a) location and sizing of S/A pair and (b) DC for first ten modes

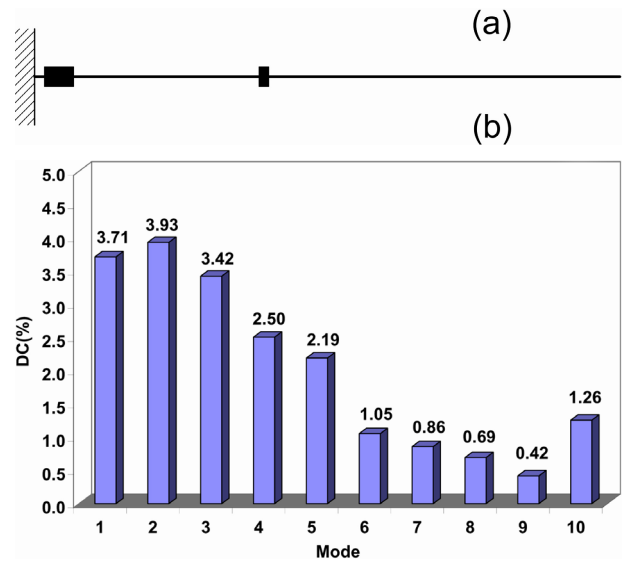


Figure 8. Two S/A pairs, DC for residual modes less than 2 %: (a) location and sizing of S/A pairs and (b) DC for first ten modes

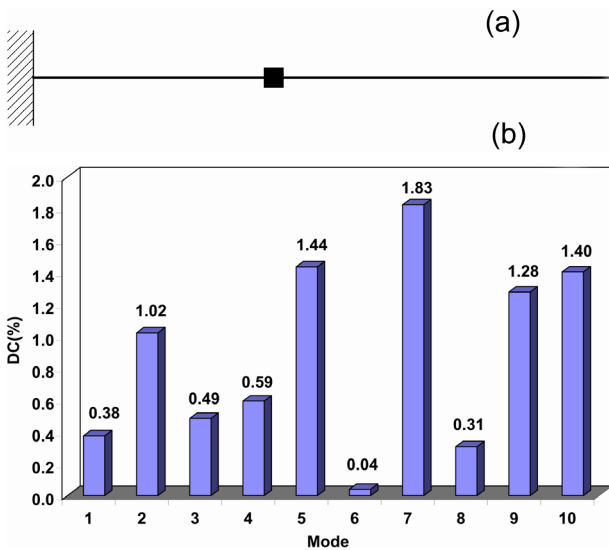


Figure 6. Single S/A pair, DC for residual modes less than 2 %: (a) location and sizing of S/A pair and (b) DC for first ten modes

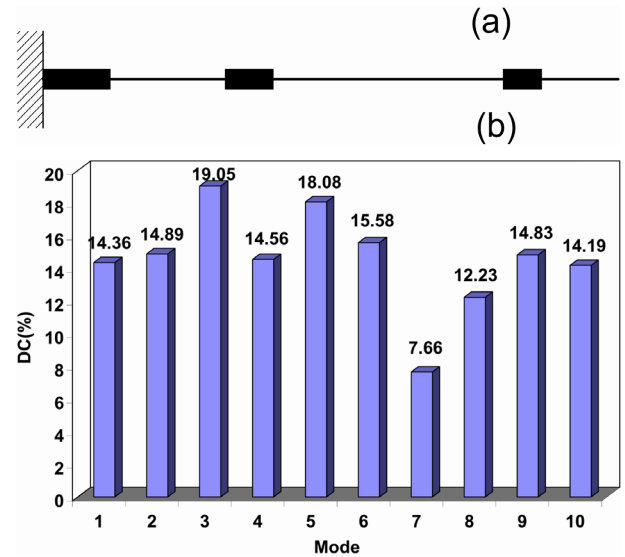


Figure 9. Three S/A pair, unconstrained DC for residual modes: (a) location and sizing of S/A pairs and (b) DC for first ten modes

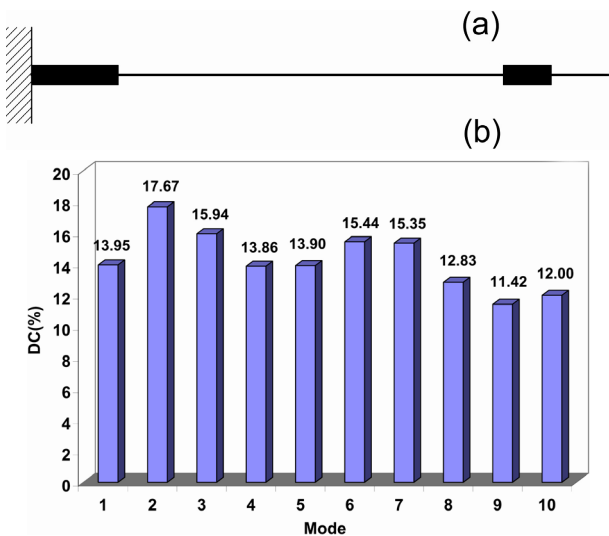


Figure 7. Two S/A pair, unconstrained DC for residual modes: (a) location and sizing of S/A pairs and (b) DC for first ten modes

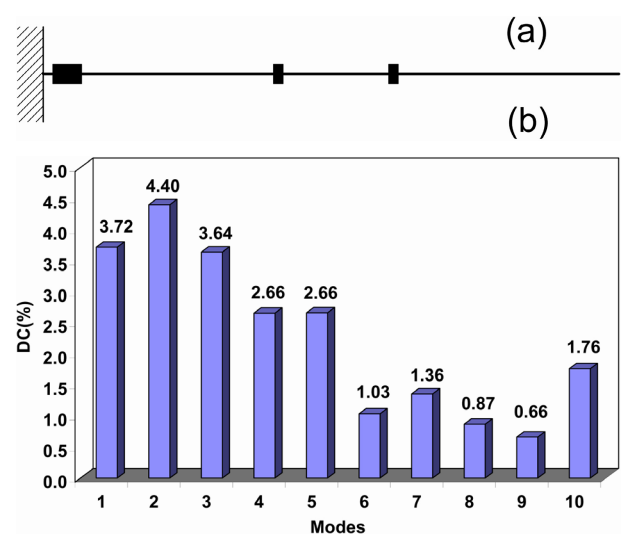
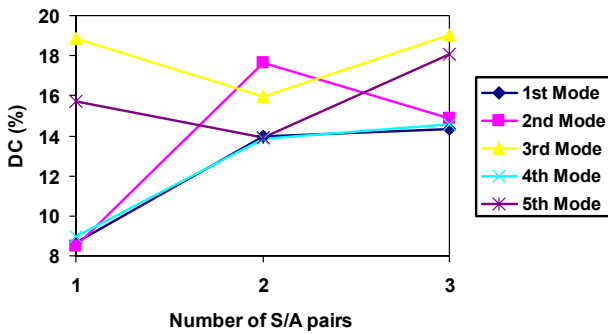


Figure 10. Three S/A pairs, DC for residual modes less than 2 %: (a) location and sizing of S/A pairs and (b) DC for first ten modes

**Table 3. Optimal sizing and location of S/A pairs**

Number of S/A pairs	Unconstrained DC for res. modes		DC for res. modes less than 2 %	
	Location [mm]	Length [mm]	Location [mm]	Length [mm]
1	120	160	220	20
2	0	90	10	30
	490	50	230	10
3	0	70	10	30
	190	50	240	10
	480	40	380	10

Comparing DCs in the case of unconstrained DC for residual modes among the number of S/A pairs (Fig. 11), it is clear that increase of the number of S/A pairs leads to increase of DCs for all modes, globally. Figure 5b shows that in the case of a single S/A pairs only two modes have a good DC, but the rest three have a low DC. In this case, DC for residual modes is very high, even higher than some controlled modes (Figs. 5b, 7b and 9b).



**Figure 11. DC for controlled modes versus number of S/A pairs for unconstrained DC for residual modes**

Keeping DC for residual modes below 2 % leads to decreasing the DC for controlled modes. For a single S/A pair, DCs for controlled modes are less than DCs for residual modes (Fig. 6b). In this case, increasing the number of S/A pairs leads to increase of DCs for controlled modes (Fig. 12).

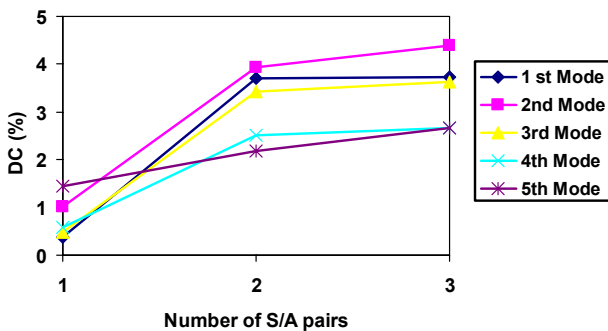


**Figure 12. DC for controlled modes versus number of S/A pairs for constrained DC for residual modes**

## 6. CONCLUSION

The degree of controllability (DC), which is used to represent control effectiveness, is defined in a such way that it possesses computational simplicity, independence of the applied control law and easy handling in the case of finite element discretization. The fuzzy set theory

implementation enables easy computation, expression simplicity of constraints and objective functions, and avoiding the use of weighing coefficients and penalty functions. Also, the particle swarm optimization technique provides fast convergence, reducing the computational time.

Although this work deals with optimization problems in the case of laminated beam, taking into account all advantages presented here, the considered optimization technique can be also studied for more complex structures.

## ACKNOWLEDGMENT

This work is supported by the Ministry of Science and Technological Development of the Republic of Serbia through Technological Development Projects No. 35035 and No. 35006.

## REFERENCES

- [1] Frecker, M.I.: Recent advances in optimization of smart structures and actuators, *Journal of Intelligent Material Systems and Structures*, Vol. 14, No. 4-5, pp. 207-216, 2003.
- [2] Gupta, V., Sharma, M. and Thakur, N.: Optimization criteria for optimal placement of piezoelectric sensors and actuators on a smart structure: A technical review, *Journal of Intelligent Material Systems and Structures*, Vol. 21, No. 12, pp. 1227-1243, 2010.
- [3] Bruant, I., Coffignal, G., Lene, F. and Verge, M.: A methodology for determination of piezoelectric actuator and sensor location on beam structures, *Journal of Sound and Vibration*, Vol. 243, No. 5, pp. 861-882, 2001.
- [4] Ramesh Kumar, K. and Narayanan, S.: The optimal location of piezoelectric actuators and sensors for vibration control of plates, *Smart Materials and Structures*, Vol. 16, No. 6, pp. 2680-2691, 2007.
- [5] Hać, A. and Liu, L.: Sensor and actuator location in motion control of flexible structures, *Journal of Sound and Vibration*, Vol. 167, No. 2, pp. 239-261, 1993.
- [6] Bruant, I., Gallimard, L. and Nikoukar, S.: Optimal piezoelectric actuator and sensor location for active vibration control, using genetic algorithm, *Journal of Sound and Vibration*, Vol. 329, No. 10, pp. 1615-1635, 2010.
- [7] Gawronski, W.: Simultaneous placement of actuators and sensors, in: *Proceedings of the 18<sup>th</sup> International Modal Analysis Conference*, 07-10.02.2000, San Antonio, USA, pp. 1474-1478.
- [8] Preumont, A.: *Vibration Control of Active Structures: An Introduction*, Kluwer Academic Publisher, Dordrecht, 2002.
- [9] Halim, D. and Moheimani, S.O.R.: An optimization approach to optimal placement of collocated piezoelectric actuators and sensors on a thin plate, *Mechatronics*, Vol. 13, No. 1, pp. 27-47, 2003.
- [10] Roy, T. and Chakraborty, D.: Optimal vibration control of smart fiber reinforced composite shell

- structures using improved genetic algorithm, *Journal of Sound and Vibration*, Vol. 319, No. 1-2, pp. 15-40, 2009.
- [11] Simões Moita, J.M., Franco Correia, V.M., Martins, P.G., Mota Soares, C.M. and Mota Soares, C.A.: Optimal design in vibration control of adaptive structures using a simulated annealing algorithm, *Composite Structures*, Vol. 75, No. 1-4, pp. 79-87, 2006.
- [12] Heyliger, P.R. and Reddy, J.N.: A higher order beam finite element for bending and vibration problems, *Journal of Sound and Vibration*, Vol. 126, No. 2, pp. 309-326, 1988.
- [13] Ballas, P.G.: *Piezoelectric Multilayer Beam Bending Actuators*, Springer-Verlag, Berlin, 2007.
- [14] Wang, Q. and Wang, C.M.: A controllability index for optimal design of piezoelectric actuators in vibration control of beam structures, *Journal of Sound and Vibration*, Vol. 242, No. 3, pp. 507-518, 2001.
- [15] Wang, S.Y., Quek, S.T. and Ang, K.K.: Vibration control of smart piezoelectric composite plates, *Smart Materials and Structures*, Vol. 10, No. 4, pp. 637-644, 2001.
- [16] Zhao, T. and Wang, X.: A multi-objective fuzzy optimization method of resource input based on genetic algorithm, *World Academy of Science, Engineering and Technology*, Vol. 69, No. 45, pp. 710-714, 2010.
- [17] Bellman, R.E. and Zadeh, L.A.: Decision-making in a fuzzy environment, *Management Science*, Vol. 17, No. 4, pp. B-141-B-164, 1970.
- [18] Kennedy, J. and Eberhart, R.: Particle swarm optimization, in: *Proceedings of the IEEE International Conference on Neural Networks*, Vol. 4, 27.11-01.12.1995, Perth, Australia, pp. 1942-1948.
- [19] Perez, R.E. and Behdinan, K.: Particle swarm approach for structural design optimization, *Computers & Structures*, Vol. 85, No. 19-20, pp. 1579-1588, 2007.
- [20] Jin, Y.-X., Cheng, H.-Z., Yan, J.Y. and Zhang, Li.: New discrete method for particle swarm optimization and its application in transmission network expansion planning, *Electric Power Systems Research*, Vol. 77, No. 3-4, pp. 227-233, 2007.

---

**ВИШЕЦИЉНА ФАЗИ ОПТИМИЗАЦИЈА  
ВЕЛИЧИНЕ И ПОЛОЖАЈА  
ПИЕЗОЕЛЕКТРИЧНИХ АКТУАТОРА И  
СЕНЗОРА**

**Немања Д. Зорић, Александар М. Симоновић,  
Зоран С. Митровић, Слободан Н. Ступар**

Овај рад представља вишециљну фазу оптимизацију величине и положаја пиезоелектричних актуатора и сензора на танкозиду композитну греду за активно управљање вибрација користећи степен управљивости (DC) контролисаних модова као критеријум оптимизације. Процес оптимизације је извршен уз ограничење промене првобитних динамичких карактеристика, укључујући ограничење у порасту масе, употребљавајући или занемарујући ограничења степена управљивости резидуалних модова за редукцију „spillover“ ефекта. Псеудоциљне функције изведене на бази теорије фазе скупова на јединствен начин дефинишу глобалне функције циља елиминишући употребу казнених функција. Проблем је дефинисан употребом методе коначних елемената базиране на „TSD“ теорији. „Particle swarm“ оптимизација је употребљена за налажење оптималне конфигурације. Неколико нумеричких примера је приказано за случај конзоле.